

Kalman Filter-Based Data Stabilization for an Automated Water Quality Monitoring System in *Macrobrachium Rosenbergii* Larvae Culture

A. Y. Yaakob, M. H. Azham, M. H. M. Ramli*
School of Mechanical Engineering, College of Engineering,
Universiti Teknologi MARA, Shah Alam, Selangor, MALAYSIA
*haniframli@uitm.edu.my

ABSTRACT

*Manual monitoring and management of water quality parameters in *Macrobrachium Rosenbergii* (freshwater prawn) larval culture are labour-intensive, time-consuming, and susceptible to human error. This research aims to develop and evaluate an automated water quality monitoring system for freshwater prawn larval culture, with a specific emphasis on data stabilization. An ESP32 microcontroller is implemented to allow remote communication using an internet connection. The system continuously monitors critical parameters using sensors such as temperature, pH, turbidity, and Total Dissolved Solids (TDS), facilitating remote real-time data acquisition. The Message Queuing Telemetry Transport (MQTT) publish-subscribe protocol is employed for seamless communication between the microcontroller and the monitoring dashboard. A Kalman filter is integrated into the system, enabling real-time sensor noise reduction and dynamic adaptation to changes. The filtered data are displayed remotely using a Node-RED dashboard with graphical representations. The implementation of the ESP32 microcontroller with the MQTT protocol and Node-RED has proven to be a robust platform for seamless data communication and presentation. Integration of the Kalman Filter significantly mitigates fluctuations in sensor readings. This is further proven by comparisons of the filtered data with known-good sensors, which have shown minimal to acceptable error percentages between 1% - 8.5%, where the error can mainly be attributed to environmental factors. Overall, this study has established a framework that can contribute to improving aquaculture practices and promoting environmental sustainability in*

freshwater prawn culture operations. The validated system provides valuable insights that assist farmers in facilitating a more efficient prawn culture operation.

Keywords: *Macrobrachium Rosenbergii; Water Quality Monitoring; ESP32 Embedded System; Total Dissolved Solids; Kalman Filter*

Introduction

Macrobrachium Rosenbergii, commonly known as the giant freshwater prawn, stands as a valuable protein source, offering a sustainable alternative to red meat consumption. Its rapid growth rate and efficient feed-to-protein conversion make it an environmentally friendly choice, complemented by its versatile flavour profile [1].

Aquaculture plays a pivotal role in the economic development of many nations, contributing significantly to global food security. Recognizing its potential, the Food and Agricultural Organization (FAO) has identified aquaculture as a key developmental pursuit, promising improved human welfare [2]. However, sustaining such growth would be challenging if reliance solely on natural resources like oceans and rivers persisted. The aquaculture industry has emerged as a critical driver of seafood production, operating within controlled environments to foster species diversity, replenish wildlife populations, and rehabilitate habitats for endangered species [3].

The advent of automated monitoring systems in aquaculture heralds a new era in environmental management, seamlessly integrating advanced technology to optimize the monitoring and control of crucial parameters. This innovative approach leverages a network of sensors, data analytics, and real-time communication to continuously assess water quality indicators such as pH, temperature, Total Dissolved Solids (TDS), and turbidity. By facilitating comprehensive data analysis, these systems empower farmers to identify potential issues, enhance operational efficiency, and ensure the well-being of aquatic organisms. Moreover, automation minimizes manual intervention while providing practitioners with valuable insights, fostering sustainable and environmentally responsible practices in aquaculture [4]-[5].

This project aims to develop and evaluate an automated monitoring system tailored for freshwater prawn culture, with a specific emphasis on achieving data stability. Conventional manual monitoring methods are not only time-consuming but also prone to inaccuracies, potentially impacting prawn growth and health. The proposed automated system will leverage state-of-the-art sensors to monitor key water quality parameters, including temperature, pH, dissolved solid levels, and turbidity. Real-time data is collected using microcontrollers and processed through a Node-RED dashboard, offering farmers and researchers precise insights.

To address the challenges of sensor noise and high data fluctuations, a Kalman filter is incorporated into the system's data processing pipeline. The Kalman filter is an optimal recursive data processing algorithm that effectively reduces errors and uncertainties from noisy sensor measurements to enhance data stability, minimizing the impact of noise and fluctuations, thereby improving the reliability and accuracy of the water quality monitoring process [6].

Optimal conditions for *Macrobrachium Rosenbergii*

Maintaining optimal conditions for freshwater prawn cultivation is essential for ensuring successful culture production. From temperature and pH levels to total dissolved solids and turbidity, each factor intricately influences the aquatic habitat.

Temperature

Temperature plays a critical role in the life cycle of the giant freshwater prawn, exerting profound effects on its metabolism, growth, and reproduction [7]. Temperatures falling within the species' optimal range are conducive to health and successful aquaculture, while extremes can induce stress, hinder growth, and impair reproduction.

Water temperature is influenced by various environmental factors, including sunlight intensity, air temperature, humidity, prawn density, and human management practices such as water exchange. *Macrobrachium Rosenbergii* exhibits remarkable adaptability to a wide range of temperatures, with an ideal temperature range typically spanning from 26 °C to 31 °C.

pH level

The pH level of water plays a significant role in the well-being of freshwater prawns, impacting enzyme activity, metabolism, and overall health [8]-[9]. Variations from the prawn's preferred neutral to slightly alkaline pH range can induce stress, impede growth, and heighten susceptibility to diseases.

pH fluctuations can result from biological activities such as prawn metabolism and microbial processes, as well as external factors like organic matter decomposition and mineral additions. Lower pH levels have been found to be detrimental to the shell quality of early juveniles and post-larvae of the giant prawn [10]. The preferred pH range for optimal growth of *Macrobrachium Rosenbergii* typically falls between 7.0 and 8.5.

Total dissolved solid

TDS in water exerts a significant influence on freshwater prawns. Elevated TDS levels, stemming from dissolved salts and minerals, can disrupt osmoregulation in prawns, inducing stress and impairing growth [11]. Furthermore, high TDS concentrations may alter water quality parameters, affecting the availability of essential nutrients and overall metabolic processes.

Conversely, excessively low TDS levels may result in inadequate mineral content, compromising the physiological functions of the prawns.

Several factors contribute to the TDS value in *Macrobrachium Rosenbergii* culture. The quality of the water source, including its natural mineral content, plays a significant role in determining TDS levels. Feeding practices and the type of feed utilized can introduce organic matter and nutrients, thereby influencing TDS concentrations. Evaporation and water exchange rates also impact TDS levels, with higher rates of evaporation potentially leading to increased TDS concentrations. Additionally, environmental factors such as temperature and pH can affect mineral solubility in water, contributing to fluctuations in TDS levels.

Elevated TDS levels may serve as indicators of water pollution or contamination, as well as an abundance of specific minerals such as calcium and magnesium. Furthermore, heightened TDS concentrations can diminish the dissolved oxygen content in water, posing challenges to the survival of aquatic life [12]. A common recommendation is around 500 ppm - 1500 ppm.

Turbidity

Turbidity, characterized by the cloudiness of water caused by suspended particles, holds significant implications for freshwater prawns. High levels of turbidity can impede light penetration, diminishing the prawns' feeding efficiency and disrupting their natural behaviour [13]. Moreover, suspended particles may serve as carriers of pathogens, heightening the risk of diseases. Additionally, elevated turbidity can reduce oxygen availability and degrade water quality, ultimately inducing stress and compromising the health of *Macrobrachium Rosenbergii* [14].

Various factors contribute to turbidity levels in aquatic environments. Activities such as water movement, bottom disturbance, or excessive feeding can resuspend sediment, increasing turbidity. Furthermore, land runoff, organic matter decomposition, and the presence of suspended particles all play roles in turbidity variations [15].

System Design

At the heart of the system lies an ESP32 microcontroller equipped with built-in Wi-Fi and Bluetooth capabilities. The sensor suite comprises Analog pH, Total Dissolved Solids (TDS), Analog Turbidity, and DS18B20 Temperature sensors, offering comprehensive monitoring of water quality parameters. While the pH and TDS sensors provide insights into chemical composition, the turbidity sensor evaluates water clarity, and the temperature sensor enables precise temperature monitoring. All sensors are wired directly to the controller as depicted in Figure 1. The microcontroller is then set up to wirelessly connect to the internet via a local Wi-Fi connection.

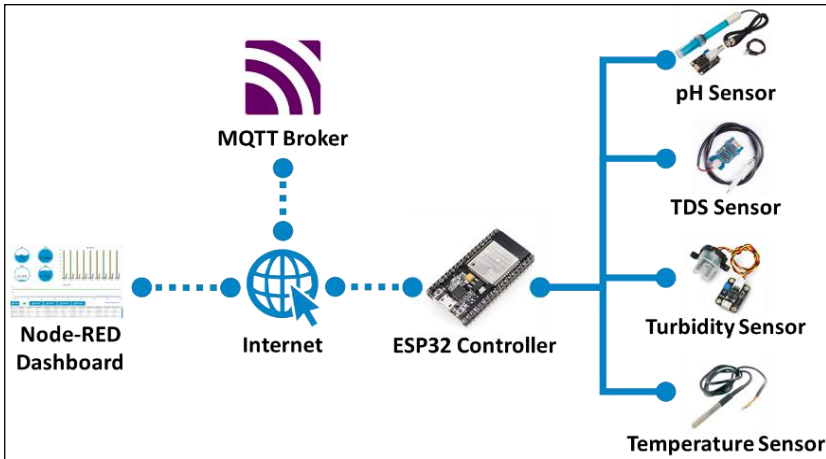


Figure 1: A simplified layout of the proposed monitoring system

Hardware implementation

The hardware setup comprised the ESP32 microcontroller and a suite of sensors optimized for efficient water parameter monitoring. Challenges were encountered during implementation, particularly in sensor calibration and addressing noise-related reliability concerns. To evaluate performance, detailed criteria focused on percentage error between sensor readings and actual values were established. Rigorous testing procedures and data analysis against predefined metrics ensured a comprehensive assessment of the hardware's functionality and performance.

ESP32 microcontroller

The ESP32 microcontroller is the core component of the monitoring system, enabling seamless communication between sensors and the Node-RED dashboard via its built-in Wi-Fi and MQTT capabilities. When paired with an expansion board, it offers additional ports, sensors, and peripherals, enhancing versatility. The expansion board incorporates an audio-like jack for external power and a micro-USB port for firmware uploads, power supply, and serial communication for programming and debugging. The ESP32's integration with an expansion board provides a flexible and robust platform for sophisticated aquaculture monitoring applications.

Analog pH sensor

The pH sensor measures solution acidity or alkalinity by detecting hydrogen ion (H⁺) concentration. It consists of a pH probe and an interface module. Key features include:

- Operates on a 3.3 V supply
- Calibrated using a potentiometer for voltage offset
- Optimal offset: 2.37 V (represents pH 7)
- Voltage range: 2.37 V - 3.3 V
- pH range: Full scale (both acidic and alkaline)

Calibration involves short-circuiting the BNC connector and adjusting the potentiometer. The 2.37 V offset allows the detection of pH values above and below 7, enabling measurement of the full pH range.

Calibrating the pH sensor is essential to ensure data accuracy. Buffer solutions as depicted in Figure 2 with known pH values (pH 4.01, pH 6.86, pH 9.18) are required for calibration and data validation. To prepare these solutions, buffer powder is mixed with 250 ml of distilled water, chosen for its high purity to avoid any influence on pH readings.

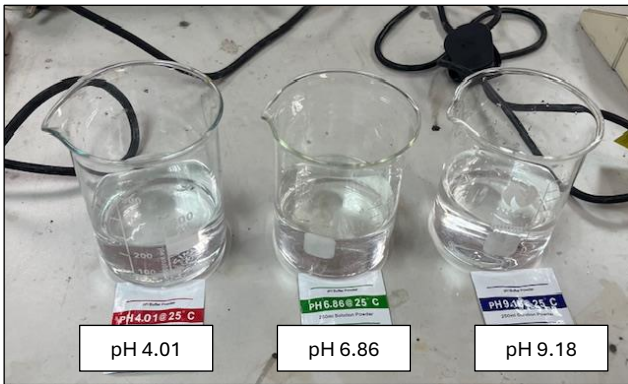


Figure 2: pH buffer solutions

Since the pH sensor is already offset at 2.37 V for pH 7, a buffer solution with a pH of 4.01 is used to obtain a voltage reading, resulting in 3.01 V. The relationship between voltage and pH value is directly proportional, allowing the determination of a constant gradient using a specific formula. This formula has been derived to calculate the pH value based on the constant gradient, m as in Equation (1):

$$pH \text{ value} = 7 - (Voltage_{pH7} - Voltage_{reading})m \quad (1)$$

To further enhance the accuracy of pH readings, additional buffer solutions with pH values of 6.86 and 9.18 are utilized to evaluate the reliability of the pH sensor. The pH probe is submerged in the pH 6.86 and pH 9.18 buffer solutions, with approximately 1 min - 2 min allowing the sensor reading to stabilize. Subsequently, the recorded pH values are recorded for analysis.

Analog Total Dissolved Solid (TDS) sensor

The TDS sensor, consisting of a probe and interface module, is connected to the ESP32 to detect dissolved solid concentrations.

Accurate readings require calibration, ideally with temperature compensation, as conductivity varies with temperature. Calibration is done by immersing the probe in a standard solution with known conductivity, about 1413 $\mu\text{S}/\text{cm}$ (~707 ppm TDS). After calibration, the sensor accurately measures water quality. To validate its performance, the sensor was tested with distilled water, tap water, and milk, and compared against readings from a commercial TDS meter (0 ppm, 108 ppm, and 85 ppm, respectively). This ensured reliability and precision.

DS18B20 temperature digital sensor

DS18B20 temperature sensor employs the 1-Wire protocol to measure its environment, simplifying wiring to only two essential lines: one for data/power and the other for ground.

To ensure data accuracy, a systematic experimental procedure is meticulously observed. First, 500 ml water is gradually heated in a container for five minutes, maintaining consistency with periodic stirring to ensure heat equilibrium. Room temperature is recorded using a commercial digital thermometer (reference reading). Subsequently, the DS18B20 temperature sensor is submerged in the heated water for two minutes (measured reading). Both reference and measured sensor readings are compared. This meticulous approach guarantees precise validation, enhancing overall experimental result accuracy.

Analog turbidity sensor

Turbidity sensor operates on the fundamental principle of measuring light transmission through a liquid medium to determine its cloudiness or turbidity. Suspended particles, such as sediment or organic matter, scatter or absorb light passing through the liquid, thereby affecting the sensor's readings.

Calibrating the turbidity sensor involves establishing both minimum and maximum reference points. The process begins with the sensor in an unobstructed sensor state, free of any liquid solution. In this condition, maximum light transmission is recorded, typically resulting in an analogue reading value of 4905. To achieve the opposite extreme, a cardboard barrier is introduced between the probe, simulating maximum turbidity, which represents 0 on the scale. To standardize these readings between a 0% - 100% range, a mapping function is employed for effective conversion, as shown in Equation (2):

$$\text{Int turbidity} = \text{map}(\text{sensorVal}, 0, 4905, 0, 100) \quad (2)$$

This function ensures a consistent and standardized representation of turbidity values across various solutions, providing a reliable metric for assessing the clarity of the liquid medium.

To validate the turbidity sensor's accuracy, experiments were conducted using four solutions: clear water, syrup water, soil-mixed water, and coffee (as depicted in Figure 3), each representing different turbidity levels. The sensor was first immersed in clear water to establish a baseline for low turbidity, followed by syrup water, soil-mixed water, and coffee, with readings documented at each stage. This process allowed for the assessment of the sensor's performance across varying turbidity conditions.

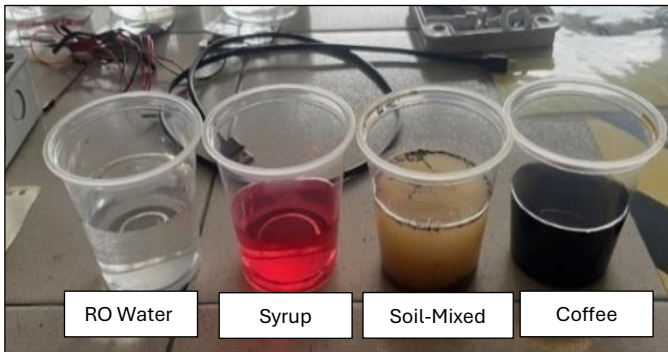


Figure 3: The different solutions used for testing the turbidity sensor (RO water, syrup, soil-mixed, and coffee)

Software environments

This study utilized two primary software tools: Arduino Integrated Development Environment (IDE) and Node-RED, which played crucial roles in sensor calibration, data processing, and visualization.

Arduino IDE

The Arduino IDE was employed to develop, test, and calibrate sensors and microcontrollers. Its extensive support for libraries simplified the integration of various sensor modules, reducing development complexity and time.

Node-RED

Node-RED was used for real-time visualization and processing of sensor data. Its flow-based programming environment allowed for dynamic monitoring and troubleshooting, making it an essential tool for managing sensor networks in our system. Node-RED's versatility and accessibility enhance the development of sensor-based applications, providing a dynamic and interactive environment

for displaying comprehensive sensor data [16]. The intuitive interface facilitated easy deployment and enhanced the flexibility of the system.

Communication protocol

For seamless data transmission, MQTT (Message Queuing Telemetry Transport) was implemented due to its efficiency in low-bandwidth and high-latency environments. Its publish/subscribe model ensured reliable, real-time communication between sensors and the monitoring system, enabling accurate and prompt data exchange. This protocol was crucial for the real-time performance of our sensor network.

Kalman filter

The Kalman filter is an adaptive algorithm that updates its estimates based on real-time measurements, continuously refining state estimates as new data comes in. This adaptability is crucial for handling varying levels of noise and fluctuations in sensor readings. The main principle of the Kalman filter is depicted in Figure 4.

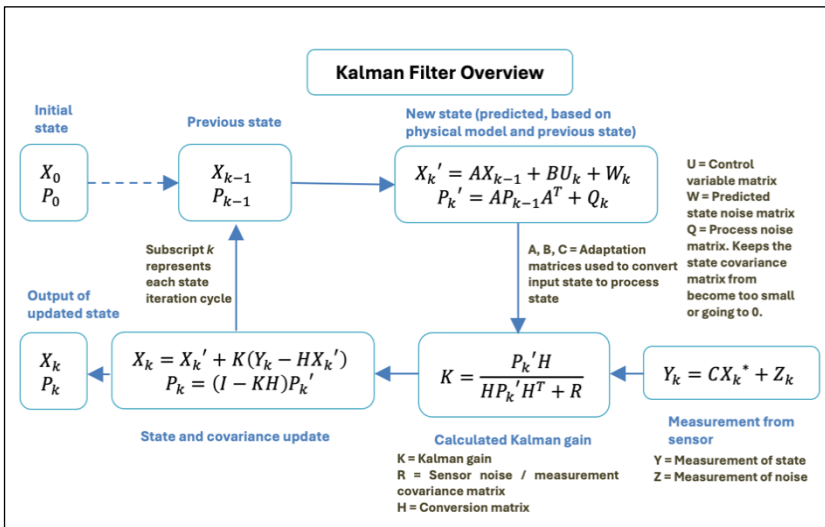


Figure 4: An overview of the Kalman filter principle

During the update phase, the Kalman filter uses a scaling factor applied to the Kalman gain. This step significantly influences the filter's decision-making process. The scaling factor, often set to a value that is very close to 1 (e.g., 1.05), governs the trade-off between trusting current measurements and relying on predictions. The updated state estimate, which reduces noise, is given by Equation (3):

$$X_e = 1.05K(P_r - Z_p) + X_p \quad (3)$$

where K is Kalman gain, P_r is current sensor reading, Z_p is the predicted measurement, and X_p is the updated state estimate.

The Kalman gain K is computed based on the predicted estimate covariance P , which determines how much the measurements influence the updated state. The estimate covariance P is updated to reduce uncertainty. This process ensures that the Kalman filter continuously refines its estimates, making it highly effective for applications requiring accurate real-time data processing in noisy environments. Finally, the new estimate X_e is calculated using the measurement P_r and K . The process noise covariance Q proportional to the process noise variance parameter, P . Adjusting Q influences the Kalman filter's responsiveness to changes in the system. A larger Q makes the filter more responsive to new measurements, while a smaller Q makes it rely more on its model predictions.

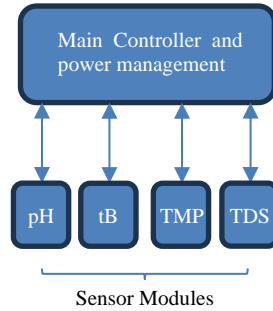
Results and Discussion

The completed prototype is depicted in Figure 5. All sensor readings are displayed using the Node-RED dashboard utilizing the MQTT messaging protocol. The ESP32's built-in Wi-Fi capabilities establish communication with the dashboard, where the ESP32 publishes data to an MQTT broker, and Node-RED subscribes to the data stream, enabling seamless data exchange over Wi-Fi. This approach demonstrates the integration of IoT technologies for effective remote monitoring [17].

Wi-Fi connectivity is the backbone of stable communication between the ESP32 and Node-RED, with the connection range contingent on the Wi-Fi coverage and signal strength within the deployment environment. Unlike previous systems limited to local LCD displays connected directly to the microcontroller, this design enables remote data access, improving system convenience and efficiency.

The Node-RED dashboard (Figure 6) further enhances functionality by offering graphical representations of historical data trends, utilizing bar and line charts for easy analysis. These visualizations empower users to track performance patterns, fluctuations, and recurring cycles. Additionally, the dashboard performs hourly data analysis, highlighting maximum and minimum values per hour, aiding in the detection of trends and identification of potential anomalies or critical events.

This system significantly improves upon traditional approaches, enabling real-time remote monitoring and historical trend analysis, making it a valuable tool for informed decision-making.



Labels:
 pH: pH sensor
 tB: Turbidity sensor
 TDS: Total Dissolved Solid sensor
 TMP: Temperature sensor

Figure 5: The completed system prototype

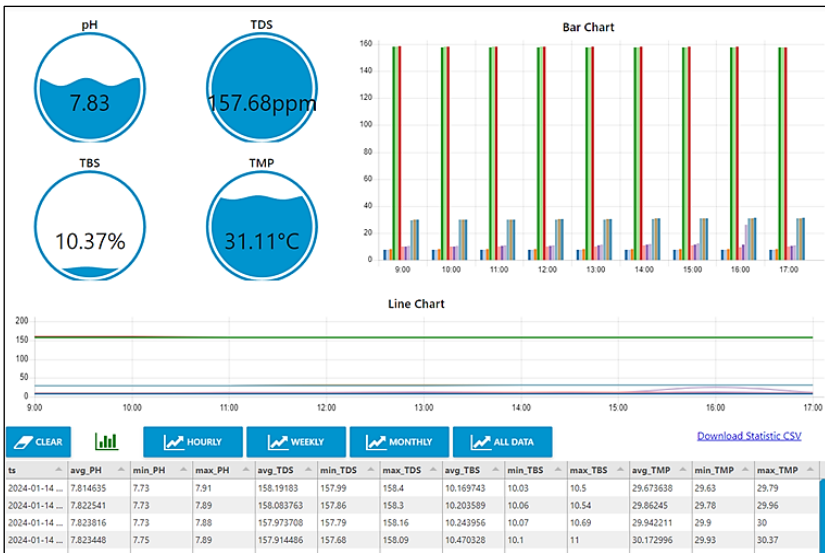


Figure 6: The snapshot of sensor readings using Node-RED dashboard

System performance

The application of the Kalman filter in our monitoring system has significantly improved the quality of sensor readings, demonstrating the filter's effectiveness in refining measurements and reducing noise. The following

results in Figures 7 to 10 highlight the substantial reduction in measurement uncertainty achieved through the Kalman filter, underscoring its ability to enhance the overall accuracy and reliability of sensor data.

Fine-tuning the process noise variance parameter Q is essential for optimizing the Kalman filter’s performance. Adjusting Q influences the filter’s responsiveness to changes in the underlying system. Higher values of Q enable quicker adaptation to new measurements, but finding the right balance is crucial. If Q is set too high, the filter may become overly sensitive to noise, reducing its effectiveness. Conversely, too low a value may cause the filter to be too slow to respond to actual changes, thus not accurately reflecting the system’s dynamics.

The Kalman filter significantly enhances system responsiveness by reducing response time during abrupt changes in sensor data, ensuring timely and accurate representation [18]. This is crucial for applications requiring real-time insights and decision-making. Evaluating the filter’s performance through standard deviation analysis reveals its noise reduction capabilities. A lower standard deviation in the filtered signal indicates effective noise mitigation, leading to more reliable estimates. Adjusting the process variance matrix Q further illustrates the filter’s impact on data stability, with standard deviation, σ_f (refer Equation 4) serving as a key metric for assessing the filter’s efficacy in reducing noise and improving sensor reading accuracy.

$$\sigma_f = \sqrt{\frac{\sum_{i=1}^N (y_{uf/f,i} - \hat{y}_{uf/f})^2}{n - 1}} \quad (4)$$

where n is the number of data points, $y_{uf/f,i}$ is the value of the unfiltered or filtered signal at instance i , and $\hat{y}_{uf/f}$ is the mean of the unfiltered or filtered signal.

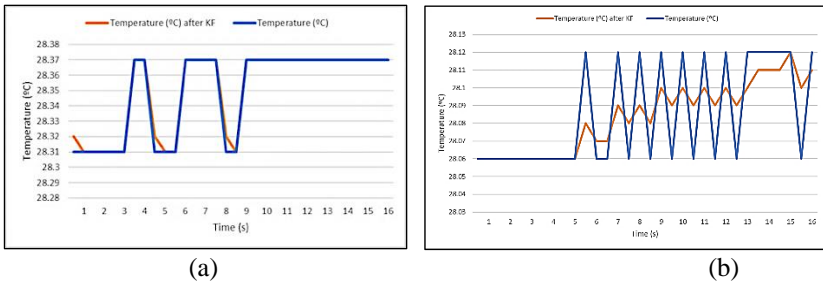


Figure 7: Temperature readings before and after the application of the Kalman filter, where (a) $Q = 0.0001$ and (b) $Q = 0.000001$

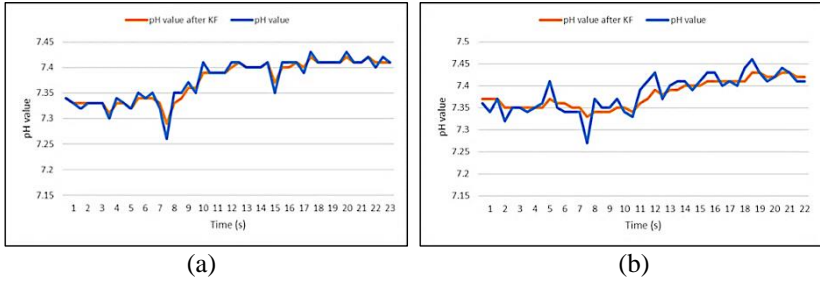


Figure 8: pH readings before and after application of the Kalman filter where (a) $Q = 0.0001$ and (b) $Q = 0.000001$

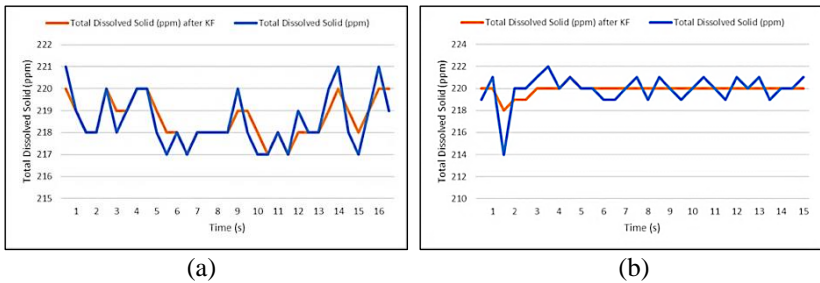


Figure 9: TDS readings before and after application of the Kalman filter where (a) $Q = 0.0001$ and (b) $Q = 0.000001$

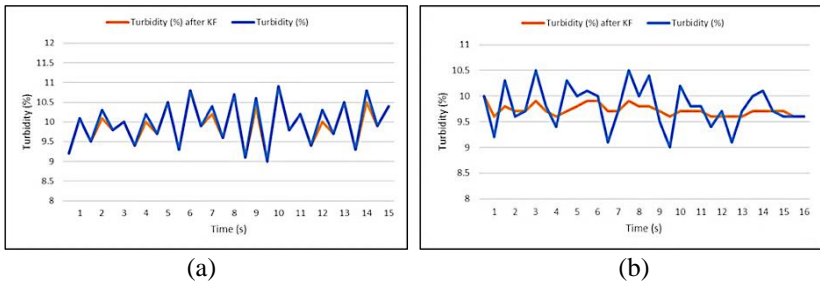


Figure 10: Turbidity readings before and after application of the Kalman filter where (a) $Q = 0.0001$ and (b) $Q = 0.000001$

Tables 1 and 2 present the standard deviation analysis for both unfiltered and KF-filtered data, considering different values of the process variance matrix, Q . The standard deviation difference between unfiltered and filtered data provides insights into the Kalman filter's efficacy in reducing noise in

different environmental parameters. For temperature, pH, TDS, and turbidity, the KF-filtered data consistently exhibits lower standard deviations compared to the unfiltered data. This reduction suggests that the Kalman filter has successfully mitigated the impact of noise, resulting in more stable and reliable measurements.

Table 1: Results of the standard deviation analysis

Data Q	Standard deviation of unfiltered data		Standard deviation of KF filtered data	
	1×10^{-4}	1×10^{-6}	1×10^{-4}	1×10^{-6}
Temperature (°C)	0.028	0.029	0.027	0.019
pH	0.041	0.040	0.038	0.031
TDS (ppm)	1.227	1.387	0.933	0.480
Turbidity (%)	0.552	0.400	0.518	0.109

Table 2: Results of the standard deviation mean analysis

Data Q	Mean of unfiltered data		Mean of KF filtered data	
	1×10^{-4}	1×10^{-6}	1×10^{-4}	1×10^{-6}
Temperature (°C)	28.34	28.08	28.35	28.08
pH	7.37	7.38	7.37	7.38
TDS (ppm)	218.54	219.93	218.60	219.9
Turbidity (%)	9.97	9.79	9.93	9.71

The process variance matrix, Q is tuned between 1×10^{-4} and 1×10^{-6} to reflect the filter's sensitivity to variations in the true system state. A smaller Q generally leads to a smoother response, as seen in the reduced standard deviations of the KF-filtered data with $Q = 1 \times 10^{-6}$. However, it is essential to strike a balance between noise reduction and preserving the original data characteristics.

Table 3 quantifies the extent of noise reduction achieved by the Kalman filter through the filtration percentage. When $Q = 1 \times 10^{-4}$, the filtration percentage is higher, indicating less aggressive filtering, while for $Q = 1 \times 10^{-6}$, the filtration percentage is lower, indicating more aggressive filtering. The choice of Q value depends on the specific application requirements and the trade-off between noise reduction and preserving the original data characteristics.

Table 3: Percentage of filtration

Data Q	Percentage of filtration (%)	
	1×10^{-4}	1×10^{-6}
Temperature (°C)	95.89	65.57
pH	92.62	77.58
Total dissolved solid (ppm)	76.06	34.63
Turbidity (%)	93.87	27.21

Validation

To ensure the reliability and accuracy of the sensor data, a comprehensive validation process was conducted through a series of experiments tailored for each sensor. The validation aimed to establish confidence in the accuracy of the generated data, ensuring the robustness and precision of the monitoring system for real-world applications.

pH sensor

The pH sensor's accuracy was evaluated using buffer solutions with known pH values. Table 4 shows the percentage errors between measured and actual pH values. The percentage error is minimal, indicating close alignment.

Certain factors may have contributed to the observed errors. Temperature variation within the laboratory environment, with a standard room temperature of 20 °C, may have influenced the accuracy of the pH readings. The optimal temperature for the buffer solutions is 25 °C, suggesting that deviations from this temperature may have impacted the measured pH values [19].

Table 4: Validation results for pH sensor

Buffer solution (pH)	Sensor reading (pH)	Error (%)
4.01	3.93	1.99
6.86	6.79	1.02
9.18	9.05	1.42

Total Dissolved Solids (TDS) sensor

Three representative solutions (distilled water, tap water, and milk) were used to assess the TDS sensor's accuracy. Readings were compared to a known-good reference sensor, where both sensors measure the same solutions at the same time. As described in Table 5, TDS readings may be influenced by external temperature, wherein the volume of water increases due to thermal expansion. This property allows more solids to be dissolved at higher temperatures [20]. A low percentage error is observed when other solutions were used, but no error for distilled water.

Table 5: Validation results for TDS sensor

Solution	Reference TDS meter (ppm)	Sensor reading (ppm)	Error (%)
Distilled water	0	0	0
Tap water	108	115	6.10
Milk	85	78	8.23

Temperature sensor

The DS18B20 Temperature Digital Sensor's reliability was evaluated at room temperature and in a mildly heated solution. Readings were compared with a calibrated digital thermometer, as compared in Table 6, revealing minor deviations attributable to environmental factors such as heat dissipation and sensor placement. A very small percentage error is observed at 1.2% and 1.5% for room temperature and heated solution respectively.

Table 6: Validation results for the temperature sensor

Solution condition	Reference thermometer (°C)	Sensor reading (°C)	Error (%)
Room temperature	20.1	19.85	1.24
Heated	35.3	34.77	1.50

Turbidity sensor

The turbidity sensor underwent testing using four liquids with varying particle levels (clear water, syrup water, water mixed with soil, and coffee), the results of which are tabulated in Table 7. The sensor effectively measured and distinguished turbidity levels, presenting readings as percentages for straightforward comparison.

Table 7: Validation results for the Turbidity sensor

Solution	Sensor reading (%)
Clear water	5
Syrup water	24
Water mixed with soil	43
Coffee	87

While minimal percentage errors were observed, the sensors demonstrated reliability in monitoring water quality and environmental conditions for *Macrobrachium Rosenbergii* aquaculture. Continued efforts to refine sensor performance and minimize errors will further enhance the effectiveness of the monitoring system in supporting sustainable aquaculture practices.

The conditions for the optimal growth of *Macrobrachium Rosenbergii* are not a fixed set of values, instead, there exists a range within which they can thrive [7]-[9]. Therefore, the minimal percentage of errors observed in these sensors is deemed acceptable, given the inherent variability is still within this range. Even with small deviations from the true values, the sensors demonstrate reliability in monitoring water quality and environmental conditions.

Moving forward, continued efforts to refine sensor performance and minimize errors will further enhance the effectiveness of the monitoring system in ensuring the well-being of aquatic ecosystems and supporting sustainable aquaculture practices.

Conclusion

The development and validation of this automated water quality monitoring system for *Macrobrachium Rosenbergii* larval culture have demonstrated the effectiveness of integrating sensors, microcontrollers, communication protocols, and data processing techniques. The comprehensive validation process, involving a series of experiments tailored for each sensor, has established confidence in the accuracy and reliability of the generated data.

The pH, Total Dissolved Solids (TDS), temperature, and turbidity sensors exhibited minimal percentage errors when compared to reference values, indicating their suitability for monitoring the critical water quality parameters essential for successful *M. Rosenbergii* aquaculture. While factors such as temperature variations, cross-contamination, and sensor positioning may have contributed to the observed errors, the sensors demonstrated reliable performance within the acceptable ranges for prawn cultivation.

Integration of the Kalman filter into the data processing pipeline played a crucial role in enhancing data stability. By effectively mitigating noise and high data fluctuations, the Kalman filter ensured more accurate and reliable sensor measurements, enabling real-time monitoring and decision-making in aquaculture operations.

The implementation of the ESP32 microcontroller, MQTT protocol, and Node-RED dashboard provided a robust and flexible platform for seamless data communication, visualization, and analysis. This system architecture paves the way for future expansions and adaptations to meet the evolving needs of aquaculture monitoring and management.

Overall, this research has established a framework for technology-enabled monitoring, contributing to improved aquaculture practices and promoting environmental sustainability in *Macrobrachium Rosenbergii* culture. The validated system offers farmers and researchers precise insights into water quality parameters, facilitating timely interventions and optimizing prawn growth and health.

Contributions of Authors

The authors confirm the equal contribution in each part of this work. All authors reviewed and approved the final version of this work.

Funding

This work received no specific grant from any funding agency.

Conflict of Interests

One of the authors, M. H. M. Ramli is a section editor of the Journal of Mechanical Engineering (JMechE). The author has no other conflict of interest to note.

Acknowledgment

The authors wish to express their profound gratitude to the College of Engineering, Universiti Teknologi MARA, for the substantial support provided throughout the course of this research. This study was made possible through the generous provision of advanced research facilities and significant financial assistance from the college.

References

- [1] I. Karplus, "Social control of growth in *Macrobrachium rosenbergii* (De Man): A review and prospects for future research", *Aquaculture Research*, vol. 36, no. 3, pp. 238-254, 2005. <https://doi.org/10.1111/j.1365-2109.2005.01239.x>
- [2] Food and Agriculture Organization of the United Nations, FAO Fisheries and Aquaculture Division, Rome, Italy: Food and Agriculture Organization of the United Nations, 2022.
- [3] A. Gupta, H. S. Sehgal and G. K. Sehgal, "Growth and carcass composition of giant freshwater prawn, *Macrobrachium rosenbergii* (De Man), fed different isonitrogenous and isocaloric diets", *Aquaculture Research*, vol. 38, no. 13, pp. 1355-1363, 2007. <https://doi.org/10.1111/j.1365-2109.2007.01787.x>

- [4] Y. Wu, Y. Duan, Y. Wei, D. An and J. Liu, "Application of intelligent and unmanned equipment in aquaculture: A review", *Computers and Electronics in Agriculture*, vol. 199, no. 1, pp. 107-201, 2022. <https://doi.org/10.1016/j.compag.2022.107201>
- [5] M. D. Ramadhona and D. L. Hakim, "System of water quality monitoring and feeding on freshwater fish cultivation," *IOP Conference Series: Materials Science and Engineering*, vol. 384, pp. 1-9, 2018. <https://doi.org/10.1088/1757-899X/384/1/012034>
- [6] A. Ma'arif, I. Iswanto, A. A. Nuryono, R. I and Alfian, "Kalman filter for noise reducer on sensor readings", *Signal and Image Processing Letters*, vol. 1, no. 2, pp. 11-22, 2019. <https://doi.org/10.31763/simple.v1i2.2>
- [7] J. Tay, A. Suhanizen, M. A. Aziz, N. Yazzin and T. Arai, "Effects of domestication and temperature on the growth and survival of the giant freshwater prawn (*Macrobrachium rosenbergii*) postlarvae", *Open Agriculture*, vol. 7, no. 1, pp. 181-190, 2022. <https://doi.org/10.1515/opag-2022-0085>
- [8] W. Cheng and J. C. Chen, "Effects of pH, temperature and salinity on immune parameters of the freshwater prawn *Macrobrachium rosenbergii*," *Fish & Shellfish Immunology*, vol. 10, no. 4, pp. 387-391, 2000. <https://doi.org/10.1006/fsim.2000.0264>
- [9] H. J. Liew, S. Rahman, P. W. Tang, K. Waiho, H. Fazhan, N. W. Rasdi, S. I. A. Hamin, S. Mazelan, S. Muda, L. S. Lim, Y. M. Chen, Y. M. Chang, L. Q. Liang and M. A. Ghaffar, "Low water pH depressed growth and early development of giant freshwater prawn *Macrobrachium rosenbergii* larvae", *Heliyon*, vol. 8, no. 7, pp. 1-12, 2022. <https://doi.org/10.1016/j.heliyon.2022.e09989>
- [10] G. Kawamura, T. Bagarinao, A. S. K. Yong, S. N. Noor and L. S. Lim, "Low pH water impairs the tactile sense of the postlarvae of the giant freshwater prawn *Macrobrachium rosenbergii*", *Tropical Life Sciences Research*, vol. 29, no. 1, pp. 103-112, 2018. <https://doi.org/10.21315/tlsr2018.29.1.7>
- [11] B. Chand, R. K. Trivedi, S. K. Dubey, S. Rout, M. M. Beg and U. Das, "Effect of salinity on survival and growth of giant freshwater prawn *Macrobrachium rosenbergii* (De Man)", *Aquaculture Reports*, vol. 2, pp. 26-33, 2015. <https://doi.org/10.1016/j.aqrep.2015.05.002>
- [12] S. R. Raja, B. Kanagaraj and S. Eunice, "Evaluating groundwater contamination: An examination of a municipal solid waste dump yard in southern India's Manchester City", *Resources, Conservation and Recycling Advances*, vol. 20, pp. 1-13, 2023. <https://doi.org/10.1016/j.rcradv.2023.200196>

- [13] G. L. Saw, "Effect of clay turbidity on the growth performance of *Macrobrachium rosenbergii* (De Man, 1897)," Department of Aquaculture, Faculty of Agriculture, Universiti Putra Malaysia Institutional Repository, Serdang, Selangor, Malaysia, Final Year Project Report, 2013.
- [14] R. Ern, D. T. T. Huong, V. C. Nguyen, T. Wang and M. Bayley, "Effects of salinity on standad metabolic rate and critical oxygen tension in the giant freshwater prawn (*Macrobrachium rosenbergii*)", *Aquaculture Research*, vol. 44, pp. 1259-1265, 2013. <https://doi.org/10.1111/j.1365-2109.2012.03129.x>
- [15] K. Adha, S. M. Long, A. S. N. A. Suhaili and F. F. Nicholas, "Fecundity of freshwater prawn (*Macrobrachium rosenbergii*) in selected rivers of Sarawak, Malaysia", *Biodiversitas Journal of Biological Diversity*, vol. 17, no. 2, pp. 498-502, 2016. <https://doi.org/10.13057/biodiv/d170215>
- [16] K. Ferencz and J. Domokos, "Using Node-RED platform in an industrial environment," *Jubileumi Kandó Konferencia*, pp. 1-12, 2020.
- [17] X. Liu, T. Zhang, N. Hu, P. Zhang and Y. Zhang, "The method of Internet of Things access and network communication based on MQTT", *Computer Communications*, vol. 153, pp. 169-176, 2020. <https://doi.org/10.1016/j.comcom.2020.01.044>.
- [18] L. C. Hun, L. Y. Ong, T. S. Lim and V. C. Koo, "Kalman Filtering and Its Real-Time Applications", in *Real-time Systems*, IntechOpen, 2016, pp. 1-180.
- [19] L. W. D. Pratami, H. G. Ariswati and D. Titisari, "Effect of temperature on pH meter based on Arduino Uno with internal calibration," *Journal of Electronics, Electromedical Engineering, and Medical Informatics*, vol. 2, no. 1, pp. 23-27, 2020. <https://doi.org/10.35882/jeeemi.v2i1.5>
- [20] W. J. Hong, N. Shamsuddin, E. Abas, R. A. Apong, Z. Masri, H. Suhaimi, S. H. Godeke and M. N. A. Noh, "Water quality monitoring with arduino based sensors", *Environments*, vol. 8, no. 1, pp. 1-15, 2021. <https://doi.org/10.3390/environments8010006>